ISSN 1063-7826, Semiconductors, 2013, Vol. 47, No. 12, pp. 1562–1566. © Pleiades Publishing, Ltd., 2013.
Original Russian Text © A.V. Germanenko, G.M. Minkov, O.E. Rut, A.A. Sherstobitov, S.A. Dvoretsky, N.N. Mikhailov, 2013, published in Fizika i Tekhnika Poluprovodnikov, 2013, Vol. 47, No. 12, pp. 1586–1590.

SYMPOSIUM "NANOPHYSICS AND NANOELECTRONICS", NIZHNI NOVGOROD, MARCH, 2013 (CONTINUATION)

Two-Dimensional Semimetal in Wide HgTe Quantum Wells: Charge-Carrier Energy Spectrum and Magnetotransport

A. V. Germanenko[a]^, G. M. Minkov[b], O. E. Rut[a], A. A. Sherstobitov[b], S. A. Dvoretsky[c], and N. N. Mikhailov[c]

[a] *Institute of Natural Sciences, Ural Federal University, Yekaterinburg, 620000 Russia*
^*e-mail: Alexander.Germanenko@usu.ru*
[b] *Institute of Metal Physics, Ural Branch, Russian Academy of Sciences, Yekaterinburg, 620990 Russia*
[c] *Institute of Semiconductor Physics, Siberian Branch, Russian Academy of Sciences, Novosibirsk, 630090 Russia*

Submitted April 22, 2013; accepted for publication April 30, 2013

Abstract—The magnetoresistivity and the Hall and Shubnikov–de Haas effects in heterostructures with a single 20.2-nm-wide quantum well made from the gapless semiconductor HgTe are studied experimentally. The measurements are performed on gated samples over a wide range of electron and hole densities. The data obtained are used to reconstruct the energy spectrum of electrons and holes in the vicinity of the extrema of the quantum-confinement subbands. It is shown that the charge-carrier dispersion relation in the investigated systems differs from that calculated within the framework of the conventional *kp* model.

DOI: 10.1134/S1063782613120063

Heterostructures with a two-dimensional electron and hole gas based on the gapless semiconductor HgTe represent a unique class of objects where fundamentally different two-dimensional (2D) systems can be implemented by varying the width of the HgTe quantum well and the composition of the $Hg_{1-x}Cd_xTe$ barriers. Thus, in a CdTe/HgTe/CdTe quantum well with a HgTe-layer thickness of $d = d_c \approx 6.5$ nm, the electron energy spectrum has no gap [1] and, for small quasimomenta k, is close to linear [2]. For $d < d_c$, the spectrum of the 2D carriers is similar to that of conventional semiconductors under quantum-confinement conditions, where the ground hole subband is formed from Γ_8 heavy-hole states and the ground electron subband is formed from Γ_6 states and light Γ_8 states. In wide quantum wells ($d > d_c$), the arrangement of the subbands is inverted, so that the lowest electron subband is formed by Γ_8 heavy-hole states (for $k = 0$) [3] and Γ_6 states contribute to the formation of the hole subbands. In recent years, the energy spectrum and electron transport in these systems have been investigated rather intensively both experimentally and theoretically [2, 4–15]. Electron systems are the most widely investigated two-dimensional systems in gapless semiconductors. Most of the experimentally observed effects can be described in this case within the framework of the conventional *kp* model. As far as the spectrum of hole states is concerned, there are currently inconsistencies both between the experimental results obtained at different times by different research teams and between experimental and theoretical results.

Here, we report experimental results on the resistivity and the Hall effect in heterostructures with a single (013)-oriented $Hg_{0.42}Cd_{0.58}Te/HgTe/Hg_{0.42}Cd_{0.58}Te$ quantum well with a nominal width of 20.2 nm. Measurements were carried out on samples shaped into Hall bars with a deposited metal electrode. This made it possible to control the conductivity and charge-carrier concentration in the quantum well over a broad range.

The typical dependences of the transverse resistivity ρ_{xy} and longitudinal resistivity ρ_{xx} on the magnetic field B for different voltages V_g applied to the gate electrode are shown in Fig. 1. One can see that, with a decrease in V_g, a change from electron conduction ($\rho_{xy} < 0$) to hole conduction ($\rho_{xy} > 0$) takes place. In addition, the following two important facts should be noted. First, in a certain range of gate voltages V_g, apart from the usual oscillatory variation in the resistivity (the Shubnikov–de Haas effect turning into the quantum Hall effect), a pronounced feature marked by vertical arrows in Figs. 1a and 1b is observed. It is clearly seen that the position of this feature is almost independent of V_g. Second, in the range of gate voltages between −3 and +1.8 V, the transverse magnetoresistance is sign-alternating (Figs. 1a, 1c); i.e., it corresponds to electron conduction in low magnetic fields and hole conduction in high magnetic fields. Together with the observation of large positive longitu-

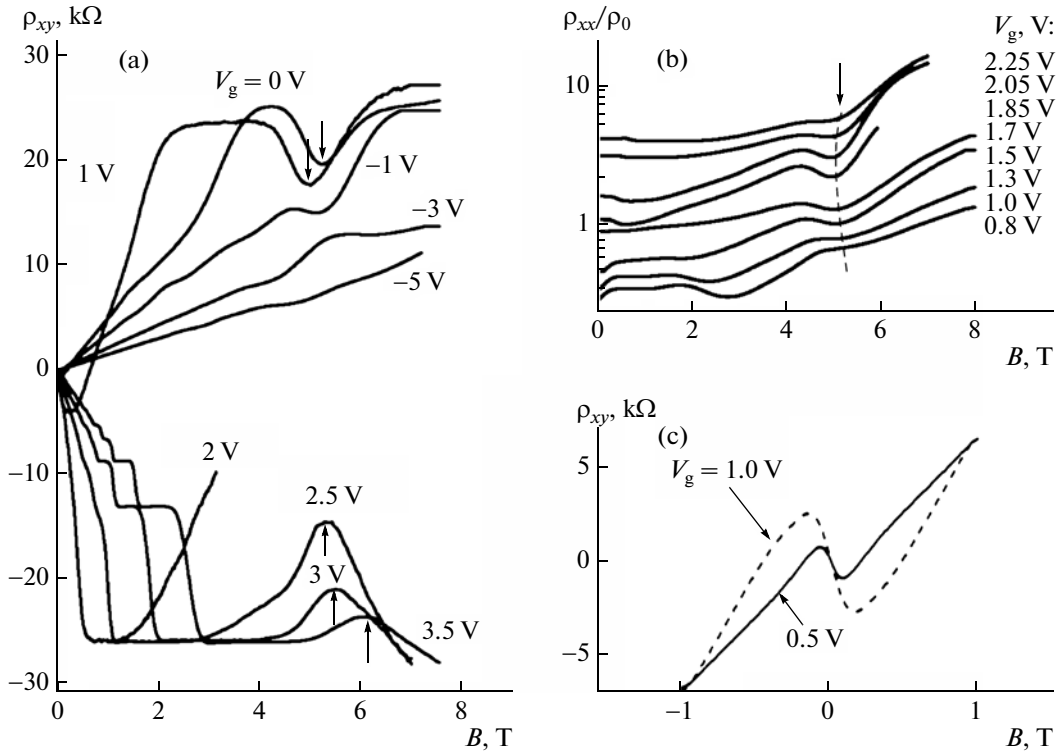

Fig. 1. Magnetic-field dependences of (a) and (c) ρ_{xy} and (b) ρ_{xx} for different voltages applied to the field electrode. The measurement temperature is $T = 1.35$ K. Vertical arrows show the feature related to the crossing of the Landau levels ($h1$, $n = 0$) and ($h2$, $n = 2$).

dinal magnetoresistance $\rho_{xx}(B)$, this fact gives unambiguous evidence that charge carriers of two or more types differing in sign of either charge or the $\partial E(k)/\partial k$ derivative (where $E(k)$ is the quasimomentum dependence of the carrier energy), which characterizes the wave-packet group velocity, participate simultaneously in the transport. The electron contribution to the Hall effect and the resistivity is retained upon a reduction in V_g to as low as −6 V, although the sign of the Hall coefficient R_H in this case corresponds to holes.

Figure 2 shows the gate-voltage dependences of the concentrations of electrons n and holes p obtained from an analysis of the behavior of $R_H(B) = \rho_{xy}(B)/B$ and $\rho_{xx}(B)$. For $V_g < 1.7$ V, this analysis was carried out within the framework of a model assuming the presence of two types of charge carriers. For $V_g > 1.7$ V, when $\rho_{xy}(B)$ and $\rho_{xx}(B)$ are determined only by electrons, their concentration was determined as $n = -1/eR_H$. It is important to note that the Hall concentrations of both electrons and holes agree within experimental uncertainty with the concentrations obtained from the period of the Shubnikov–de Haas oscillations, which were clearly observed for $V_g < 0$ and $V_g > 2.5$ V. One can see that the concentration of electrons differs from zero in the entire range of gate voltages. It should be mentioned that n is more than 100 times lower than p for the lowest gate voltage of $V_g = -6$ V. According to Fig. 2b, the dependence $n(V_g)$ is rather complicated. Three regions can be distinguished in this dependence. The performed analysis demonstrates that each of these regions corresponds to a particular position of the Fermi level E_F with respect to the band edges. This is illustrated in Fig. 3, the left-hand part of which shows the dispersion curves $E(k)$ calculated within the context of the six-band isotropic kp model by direct integration [16] using the parameters given in [17, 18]. In region A ($V_g > 1.8$ V), the Fermi level lies high in the conduction band (see Fig. 3) and only conduction-band electrons participate in the transport.

As the gate voltage decreases, the Fermi level touches the top of the valence band for $V_g \approx 1.8$ V, and, with a further decrease in V_g, falls in the region of overlap between the valence and conduction bands, where the rate of variation in $n(V_g)$ is determined by the larger density of states of the valence band. This is region B, corresponding to $V_g = 1.8$–1.0 V. Here, three types of charge carriers participate in the transport. These are electrons in the conduction band $h1$ and two types of charge carriers from the band $h2$ with electron- and hole-type curvature of the spectrum. Note that, strictly speaking, the values of n shown in Fig. 2b for this region of gate voltages do not correspond to the

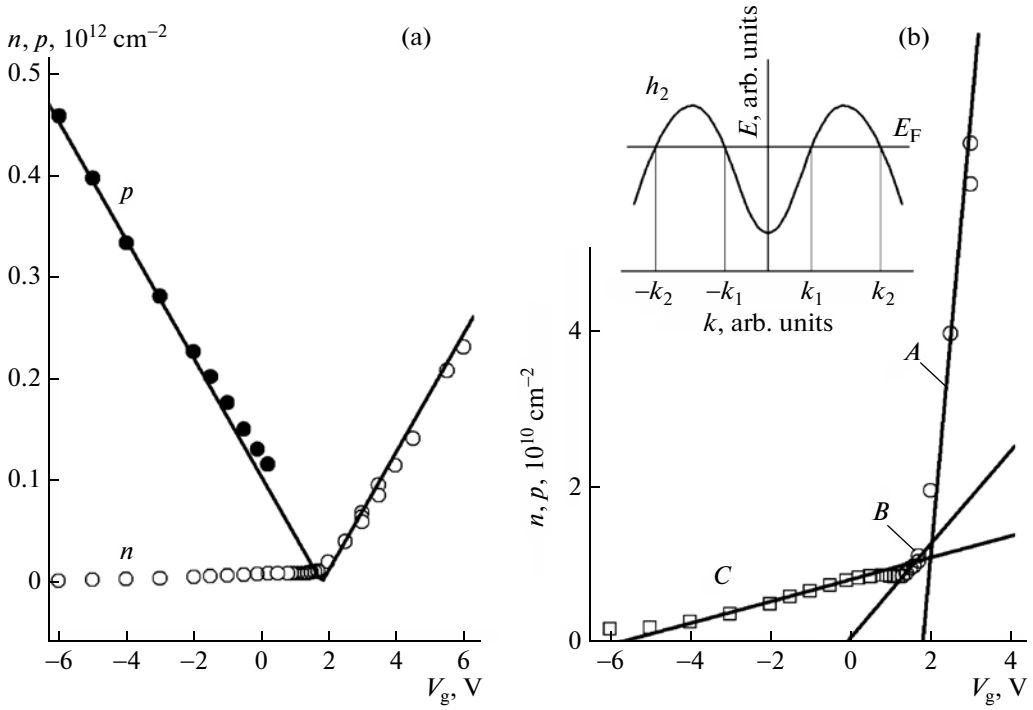

Fig. 2. (a) Dependences of the electron and hole concentrations on the gate voltage V_g. Dots show experimental points, and the solid line shows the dependence of $C|V_g - 1.8\ \text{V}|/e$ on V_g (here, $C = 9.1$ nF/cm^2 is the experimentally measured capacitance between the gate and the two-dimensional gas). (b) $n(V_g)$ dependence on an expanded scale illustrating the existence of three regions with different slopes. The inset shows the schematic layout of the dispersion relation $E(k)$ of the subband $h2$ and the position of the Fermi level corresponding to region C.

concentration of any charge carriers, in as far as only two carrier types were taken into account in the analysis of the behavior of $R_H(B)$ and $\rho_{xx}(B)$.

Finally, region C ($-6.0 < V_g < 1$ V) corresponds to a situation where the Fermi level lies below the bottom of the conduction band. The regions of the dispersion curve $E(k)$ of the subband $h2$ with hole-type and electron-type curvature add hole and electron contributions to the Hall effect, respectively. Assuming that the spectrum is isotropic, we find that the values of n and p determined from analysis of the magnetic-field dependences of ρ_{xy} and ρ_{xx} correspond in this case to the number of states within circles with the radii k_1 and k_2, where k_1 and k_2 are Fermi quasimomenta corresponding to the two regions of the $E(k)$ curve shown in Fig. 2 (see inset) [19]; thus, $n = k_1^2/2\pi$ and $p = k_2^2/2\pi$.

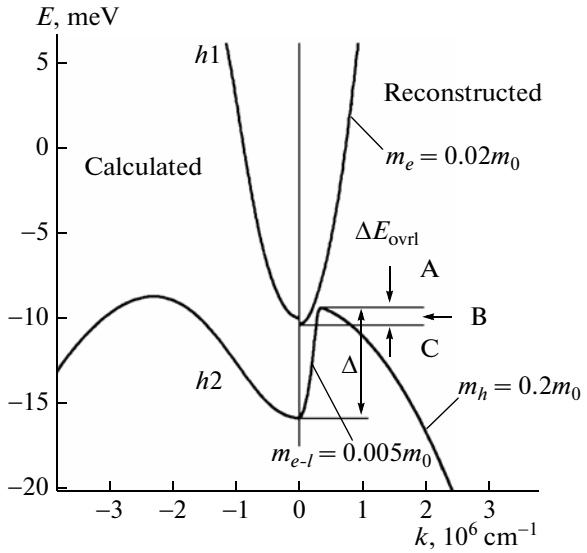

Fig. 3. Dispersion relation $E(k)$ calculated within the context of the six-band kp model (left) and reconstructed according to the experimental data (right).

The outlined picture of the spectrum is confirmed by the data on $\rho_{xx}(B)$ oscillations. The positions of the oscillation minima in the $\rho_{xx}(B)$ dependences are shown in coordinates (B, V_g) in Fig. 4. Two series of oscillations, representing the contributions from electrons and holes, are clearly seen. The corresponding charge-carrier concentrations can be determined from the oscillation periods, and the values thus obtained are in good agreement with the data in Fig. 2.

Thus, the experimental results presented above are in qualitative agreement with the calculated spectrum. However, our data make it possible to obtain the quantitative characteristics of the spectrum and perform a more detailed quantitative analysis.

The effective masses of electrons m_e and holes m_h can be determined from the analysis of the temperature dependences of the Shubnikov–de Haas-oscillation amplitude. It was found that, within experimental error (~20%), they are independent of the carrier concentrations and are equal to $m_e = 0.02m_0$ and $m_h = 0.2m_0$.

The electron effective mass obtained experimantally is close to the theoretical value. This is clearly seen in Fig. 3: the $h1$ electron branch on the left-hand and right-hand parts of the plot have similar curvatures.

The comparison of the experimental and theoretical values of the hole effective mass requires a more subtle approach, because the dispersion of the $h2$ hole subband is nonmonotonic. According to the calculations, the maximum (or, more exactly, the circle of maxima) should occur at $k \approx 2.2 \times 10^6$ cm^{-1} (left-hand part of Fig. 3). However, one can see from the fan diagram in Fig. 4 that hole-type oscillations are observed beginning from $V_g \approx 0.8$ V, i.e., $p \approx 0.5 \times 10^{11}$ cm^{-2}. In the case of isotropic dispersion, this corresponds to $k \approx 0.5 \times 10^6$ cm^{-1}. Thus, the region of the $h2$ subband dispersion curve with hole-type curvature starts from values of $k < 0.5 \times 10^6$ cm^{-1}.

Using the experimentally determined values of m_e and m_h, we can estimate such characteristic parameters of the energy spectrum as the magnitude ΔE_{ovrl} of the overlap between the $h1$ and $h2$ subbands, the depth of the central minimum Δ of the subband $h2$, and the density-of-states effective mass at this minimum m_{e-l}. Indeed, since a kink in the $n(V_g)$ dependence between regions A and B at $V_g \approx 1.8$ V occurs when the Fermi level touches the top of the $h2$ subband, the overlap can be estimated as $\Delta E_{ovrl} = \pi\hbar^2 n(1.9\text{ V})/m_e$. Using $m_e = 0.02m_0$ and $n(1.8\text{ V}) = 1.3 \times 10^{10}$ cm^{-2}, we obtain $\Delta E_{ovrl} \approx 1$ meV. Furthermore, given the value of m_h, we can estimate the depth of the central minimum Δ in the following way. This depth is approximately equal to the Fermi energy (measured from the top of the valence band) for the gate voltage $V_g = -6$ V, i.e., the voltage at which curve C in Fig. 2b intersects the horizontal axis V_g. This corresponds to the situation where the Fermi level touches the bottom of the central minimum of subband $h2$ and the electron contribution disappears and hence $\Delta = \pi\hbar^2 p(-6\text{ V})/m_h$. For $m_h = 0.2m_0$ and $p(-6\text{ V}) = 4.5 \times 10^{11}$ cm^{-2}, we obtain $\Delta \approx 5$ meV. Finally, given the value of Δ and the concentration n corresponding to $V_g = 1$ V (i.e., the gate voltage at which the Fermi level crosses the bottom of the conduction band, so that, for $V_g < 0$, the electron contribution originates solely from the minimum in the spectrum of the $h2$ subband), we can estimate m_{e-l}: $m_{e-l} = -\pi\hbar^2 n(0\text{ V})/\Delta \approx -0.005m_0$ (the negative sign corresponds to the electron-type curvature in the hole spectrum). It is important to note that the value of $0.005m_0$ is much smaller than the theoretical value, which, in the isotropic approximation, exceeds $0.1m_0$.

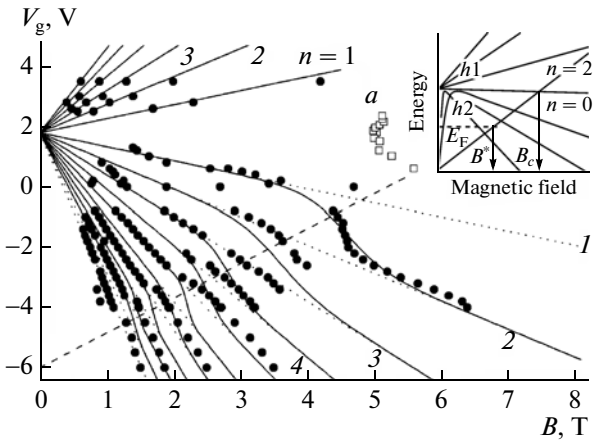

Fig. 4. Positions of the minima in the $\rho_{xx}(B)$ dependences in coordinates (B, V_g). The group of points designated as a shows the position of the minimum marked by arrows in Figs. 1a and 1b. The dashed line corresponds to the intersection of the Fermi level with the Landau level ($h2$, $n = 2$). Solid lines show the expected behavior of the minima. The inset shows the schematic diagram of the Landau levels for the $h1$ and $h2$ subbands.

The spectrum of the subbands $h1$ and $h2$ reconstructed using the values of ΔE_{ovrl}, Δ, and m_{e-l}, m_e, m_h given above is plotted on the right-hand side of Fig. 3. Evidently, this spectrum differs considerably from the calculated one, shown on the left-hand side of the same figure.

Now, let us consider the behavior of the oscillation peaks upon a variation in the gate voltage V_g; the analysis of this behavior gives some support to the above estimates. In the fan diagram of Fig. 4, there is a group of "extra" points (marked a) in the range of magnetic fields around ~5 T and voltages of $V_g = 0.5$–2 V. These points correspond to the minima marked by arrows in Fig. 1. The analysis of the Landau-level spectrum [8, 20] suggests that this feature corresponds to the case where the Fermi level appears in the region of crossing between the Landau levels ($h1$, $n = 0$) and ($h2$, $n = 2$), which occurs in a field B_c (see Fig. 4, inset). The level ($h2$, $n = 2$) starts at $B = 0$ from the energy corresponding to the minimum of the $h2$ hole subband dispersion curve. Thus, connecting the point with coordinates ($B = 0$, $V_g = -6$ V), which corresponds to the situation where the Fermi level crosses the valence-band minimum, and the point ($B = 5$ T, $V_g = 0$), we obtain an approximate gate-voltage dependence for the magnetic field B^* in which the Landau level ($h2$, $n = 2$) crosses the Fermi level (the dashed line in Fig. 4). One can see that this is exactly the region where the minima positions skip from one level number to another, as shown by the solid lines in Fig. 4.

Thus, the energy spectrum of the uppermost hole quantum-confinement subband $h2$ in wide quantum

wells based on the gapless semiconductor HgTe reconstructed according to our experimental results differs considerably from the calculated one. Analysis of the experimental data demonstrates that a narrow minimum exists at the center of the subband. The depth of this minimum is ~5 meV and the estimated effective mass is ~$0.005m_0$.

ACKNOWLEDGMENTS

This study was supported in part by the Russian Foundation for Basic Research (project nos. 12-02-00098, 13-02-00322).

REFERENCES

1. L. G. Gerchikov and A. Subashiev, Phys. Status Solidi B **160**, 443 (1990).
2. B. A. Bernevig, T. L. Hughes, and S.-C. Zhang, Science **314**, 1757 (2006).
3. M. I. D'yakonov and A. V. Khaetskii, Sov. Phys. JETP **55**, 917 (1982).
4. G. Landwehr, J. Gerschütz, S. Oehling, A. Pfeuffer-Jeschke, V. Latussek, and C. R. Becker, Physica E **6**, 713 (2000).
5. X. C. Zhang, A. Pfeuffer-Jeschke, K. Ortner, C. R. Becker, and G. Landwehr, Phys. Rev. B **65**, 045324 (2002).
6. K. Ortner, X. C. Zhang, A. Pfeuffer-Jeschke, C. R. Becker, G. Landwehr, and L. W. Molenkamp, Phys. Rev. B **66**, 075322 (2002).
7. X. C. Zhang, K. Ortner, A. Pfeuffer-Jeschke, C. R. Becker, and G. Landwehr, Phys. Rev. B **69**, 115340 (2004).
8. M. König, S. Wiedmann, C. Brüne, A. Roth, H. Buhmann, L. W. Molenkamp, X.-L. Qi, and S.-C. Zhang, Science **318**, 766 (2007).
9. G. M. Gusev, Z. D. Kvon, O. A. Shegai, N. N. Mikhailov, S. A. Dvoretsky, and J. C. Portal, Phys. Rev. B **84**, 121302 (2011).
10. Z. D. Kvon, E. B. Olshanetsky, E. G. Novik, D. A. Kozlov, N. N. Mikhailov, I. O. Parm, and S. A. Dvoretsky, Phys. Rev. B **83**, 193304 (2011).
11. G. Tkachov and E. M. Hankiewicz, Phys. Rev. B **84**, 035444 (2011).
12. J. W. Nicklas and J. W. Wilkins, Phys. Rev. B **84**, 121308 (2011).
13. P. M. Ostrovsky, I. V. Gornyi, and A. D. Mirlin, Phys. Rev. B **86**, 125323 (2012).
14. M. S. Zholudev, A. V. Ikonnikov, F. Teppe, M. Orlita, K. V. Maremyanin, K. E. Spirin, V. I. Gavrilenko, W. Knap, S. A. Dvoretskiy, and N. N. Mihailov, Nanoscale Res. Lett. **7**, 534 (2012).
15. A. A. Greshnov, Yu. B. Vasil'ev, N. N. Mikhailov, G. Yu. Vasil'ev, and D. Smirnov, Pis'ma Zh. Eksp. Teor. Fiz. **97**, 108 (2013).
16. V. A. Larionova and A. V. Germanenko, Phys. Rev. B **55**, 13062 (1997).
17. X. C. Zhang, A. Pfeuffer-Jeschke, K. Ortner, V. Hock, H. Buhmann, C. R. Becker, and G. Landwehr, Phys. Rev. B **63**, 245305 (2001).
18. E. G. Novik, A. Pfeuffer-Jeschke, T. Jungwirth, V. Latussek, C. R. Becker, G. Landwehr, H. Buhmann, and L. W. Molenkamp, Phys. Rev. B **72**, 035321 (2005).
19. B. M. Askerov, *Electron Transport Phenomena in Semiconductors* (Nauka, Moscow, 1985; World Scientific, Singapore, 1994).
20. M. Schultz, U. Merkt, A. Sonntag, U. Rössler, R. Winkler, T. Colin, P. Helgesen, T. Skauli, and S. Lovold, Phys. Rev. B **57**, 14772 (1998).

Translated by M. Skorikov